Biomedical Signal Processing and Control 58 (2020) 101865

Contents lists available at ScienceDirect

Biomedical Signal Processing and Control

journal homepage: www.elsevier.com/locate/bspc

A new method for muscular visual fatigue detection using electrooculogram

Mengchuang Song[a,b,1], Lina Li[a,b,1], Jintao Guo[a,b], Tian Liu[a,b,*], Shuyin Li[a,b], Yingtuo Wang[a,b], Qurat ul ain[a,b], Jue Wang[a,b,*]

[a] The Key Laboratory of Biomedical Information Engineering of Ministry of Education, The Key Laboratory of Neuro-informatics & Rehabilitation Engineering of Ministry of Civil Affairs, and Institute of Health and Rehabilitation Science, School of Life Science and Technology, Xi'an Jiaotong University, Xianning West Road 28#, Xi'an 710049, Shaanxi, PR China

[b] National Engineering Research Center of Health Care and Medical Devices, School of Life Science and Technology, Xi'an Jiaotong University, Xianning West Road 28#, Xi'an 710049, Shaanxi, PR China

ARTICLE INFO

Article history:
Received 30 September 2019
Received in revised form 6 December 2019
Accepted 19 January 2020

Keywords:
Critical fusion frequency
Electrooculogram physiological indicators
Support vector machine classifying
Muscular visual fatigue detection

ABSTRACT

Objective: Muscular visual fatigue (MVF)is increasingly common in clinic; However, there is no objective and effective means for the detection of muscular visual fatigue. This study focuses on a new method for muscular visual fatigue detection based on electrooculogram (EOG).
Methods: We analyzed the mechanism that develops muscular visual fatigue and designed an experiment to induce muscular visual fatigue intentionally. And we recorded electrooculogram and critical fusion frequency (CFF) in the process. Then we got four electrooculogram physiological indicators and correlation between them and critical fusion frequency was analyzed. Finally, the indicators tendency, statistical difference and support vector machine (SVM) analysis were carried out.
Results: The work shows that both wavelet packet barycenter frequency (WPBF) and average blink time (ABT) are significantly correlated with critical fusion frequency, tendency of both them has a good consistency, there is a significant difference for them both before and after muscular visual fatigue and that the trained support vector machine has a classification accuracy of 0.796 (SD 0.172) for states before and after muscular visual fatigue.
Conclusion: Wavelet packet barycenter frequency and average blink time can be used for muscular visual fatigue detection, a certain degree of muscular visual fatigue occurred after induction and the trained support vector machine can achieve a good classification detection. We conclude that wavelet packet barycenter frequency and average blink time can be used for accurate muscular visual fatigue detection.
Significance: This study is of great significance in muscular visual fatigue prevention and treatment.

1. Background

Visual fatigue refers to the excessive tension of the visual organs over a long time, which is over its compensation ability to cause a group of ocular and systemic symptoms [1]. With the popularity of video terminals such as computers, the morbidity of visual fatigue is increasing year by year [2]. Visual fatigue is closely related to the health condition of one's physiology & psychology, and it's also related to various optic impairments. Therefore, it is clinically known as visual fatigue syndrome [3]. Ocular factors including dry eye, refractive error, muscle force imbalance, binocular visual dysfunction and other eye diseases contribute greatly in causing visual

Abbreviations: CFF, Critical Fusion Frequency; MVF, Muscular Visual Fatigue; EOG, Electrooculogram; ERLH, Energy Ratio of Low Frequency to High Frequency; WPBF, Wavelet Packet Barycenter Frequency; ABT, Average Blink Time; ABE, Average Blink Energy; rERLH, Correlation Coefficient between CFF and ERLH; rWPBF, Correlation Coefficient between CFF and WPBF; rABT, Correlation Coefficient between CFF and ABT; rABE, Correlation Coefficient between CFF and ABE; SVM, Support Vector Machine; SD, Standard Deviation; HARS, The Hamilton Anxiety Rating Scale; VDT, Video Display Terminals; SNR, Signal-to-Noise Ratio; VEOG, Vertical Electrooculogram; HEOG, Horizontal Electrooculogram; NS_WPBF, Normalized and Standardized WPBF; NS_ABT, Normalized and Standardized ABT; RBF, Radial Basis Function; ROC, Receiver Operating Characteristic Curve; AUC, Area under Curve; PST, Paired Sample T Test; MF, Median Frequency; EMG, Electromyography.

* Corresponding author at: The Key Laboratory of Biomedical Information Engineering of Ministry of Education, The Key Laboratory of Neuro-informatics & Rehabilitation Engineering of Ministry of Civil Affairs, and Institute of Health and Rehabilitation Science, School of Life Science and Technology, Xi'an Jiaotong University, Xianning West Road 28#, Xi'an 710049, Shaanxi, PR China.
E-mail addresses: chuang948507541@stu.xjtu.edu.cn (M. Song), lla2017@stu.xjtu.edu.cn (L. Li), guojintao2016@stu.xjtu.edu.cn (J. Guo), tianliu@xjtu.edu.cn (T. Liu), li_shuyin@qq.com (S. Li), 1505691570@qq.com (Y. Wang), qurat.iimc@gmail.com (Qurat ul ain), juewang_xjtu@126.com (J. Wang).
[1] These authors contributed equally to this work.

https://doi.org/10.1016/j.bspc.2020.101865
1746-8094/

fatigue. Physical factors include physical health and disease. The psychological factors chiefly include mental state, personal character and interpersonal relationship. Moreover, some scholars believe that environmental factors also lead to visual fatigue, including illumination brightness, background brightness, air environment and temperature [4]. Among all these causes of visual fatigue, ocular muscle force imbalance is more common in clinic. In most cases, ocular muscle force imbalance can lead to MVF [5].

MVF is a type of visual fatigue in which long term extraocular muscle imbalance or excessive tension in the motor supply of optic nerve causes fatigue. The sufferer often experience exophoria and convergence insufficiency, with symptoms such as reading unsustainably, unclear vision, diplopia, eye irritation, headache, dizziness, nausea [6] etc. Due to the lack of symptoms specificity, it is often misdiagnosed as refractive error, glaucoma, neurasthenia, vascular headache or other related dysfunctions. The dysfunction of convergence often leads to the imbalance of the extraocular muscle strength affecting the eye position and results in phoria. If the level of phoria is low, eye position can be compensated by small convergence thereby correcting phoria. However, when the phoria level is over high or the convergence reserve is insufficient, MVF will occur [7]. MVF caused by convergence insufficiency is pretty common in clinic, and the morbidity is relatively high [8]. What's more, the morbidity of teenagers between the ages of 7 and 13 is much higher [9,10]. Cooper's work has focused on different convergence effects during close work and found that MVF is related to convergence function, he concluded that long time close work will decrease the sensitivity of convergence [11]. In addition, eye accommodation is mainly achieved by the ciliary muscle and the convergence function is completed through the cooperation of the extraocular muscles. As we know that eye accommodation and convergence are related to each other, so eye fatigue caused by refractive error or visual dysfunction is related to both the intraocular and extraocular muscles and it can collectively be called ocular MVF [5]. Researchers have proved that under heavy visual burden, people will suffer from cognitive fatigue and visual fatigue [12,13]. Meanwhile, it is reported that some methods can be used to assess visual fatigue.

So far, many methods of visual fatigue assessment have been reported in ophthalmology research. Takahashi has found that CFF, as an objective behavioral indicator, is negatively correlated with visual fatigue [14]. CFF is well accepted as an objective behavioral indicator for visual fatigue assessment. In addition to this method, by advising and recording the patient's chief complaints along with their feelings, researchers could get the Hamilton Anxiety Rating Scale (HARS) result [15]. However, as a subjective method, in some cases HARS can't achieve a reasonable assessment. Therefore, ECG and pulse characteristics are applied to evaluate visual fatigue caused by Video Display Terminals (VDT) fatigue test [16]. We also found that, EEG is widely used to assess visual fatigue. Chen chose EEG power spectral parameters to assess visual fatigue caused by watching 3D TV in his study [17]. Zou tried to assess visual fatigue caused by convergence-accommodation conflict using EEG [18]. In addition, EOG and EEG were analyzed in Huo's research of driving fatigue [19], in their study, ECG↘EEG or EOG was applied to assess visual fatigue caused mainly by cognitive fatigue, not ocular muscular fatigue. Beyond these methods, studies have also shown that eye movement indicators such as blink rate, eye saccade speed and pupil diameter can be used for the detection and evaluation of visual fatigue [20]. As we know, eye movement reflects the physiological state of eyes, and EOG is the most direct way to show the state of eye movement. EOG shows the resting potential between the cornea and retina. When the eyeball rotates, there is a slight potential change in the epidermis around the eye. This potential change can be collected by electrodes placed around the human eye. Generally, the amplitude of EOG ranges from 0.4 to 10 mV, and the frequency varies from 0.1 to 38 Hz, and its main frequency component is below 10 Hz [21]. In some way EOG is a kind of electromyography around eyes, so EOG is closely related to MVF. In our study, we tried to find a new method for accurate MVF detection using physiological indicators based on EOG.

How to achieve an accurate detection and evaluation of ocular muscular fatigue is of great significance to detection and prevent for MVF in time. In order to achieve this goal, based on the above analysis, we proposed an assumption that certain physiological indicators based on EOG could be used for an accurate detection and evaluation of MVF. Then considering the clinically common symptoms of exophoria and convergence insufficiency, we conducted a specialized experiment and recorded the EOG signal and CFF values. This whole experimental process is shown in Fig. 1. Finally, through data process, statistical analysis and SVM research, we managed to verify our hypothesis.

2. Materials and methods

2.1. Participants

Twenty-eight visually normal, asymptomatic college students were recruited, between the age of 21 and 26 (mean age: 23), 22 males and 6 females. All participants were prohibited from drinking alcohol and taking drugs within 48 h before the experiment. They also had adequate rest for their eyes and were not having parachromatoblepsia. The convergence or accommodative function of everyone was intact or corrective. Their visual acuity was measured by automatic optical refractometer, including both emmetropes (n = 8) having a spherical equivalent refractive range of −0.5 D to +0.5 D and myopes (n = 20) with a spherical equivalent refractive range of −1.5 D to −5.00 D; and the astigmatism of all subjects was <1D. The subjects with corrected visual acuity of greater than 0.8 were included in the study. Informed consent was obtained from all participants, according to the Declaration of Helsinki. The ethics committee of the School of life science and technology at Xi'an Jiaotong University approved the study.

2.2. Experiment design

We made a pair of prism. It is base-out and the degree is adjustable. Its appearance is shown in Fig. 1(a). The whole experiment was performed in a shielded room where the environment was quiet and comfortable; the experiment procedure is shown in dotted box Fig. 1(b). Firstly, CFF was measured (subjects wearing their own corrective glasses) and EOG was recorded for 6 min before MVF. Then to induce ocular muscle fatigue, subjects were asked to watch a vertical black line of size 10 × 1.5 cm (Fig. 1(c)) shown on screen at the distance of 80 cm. In order to ensure that the subjects have normal visual function, they were asked to wear the prism and their corrective glasses at the same time. The prism was slowly adjusted to force the participants' eyes to become physiologically diplopia, and slowly continued to increase the prism degree, so that they couldn't restore the binocular single vision. Then the participants maintained this status for 12 min to form ocular muscle fatigue as much as possible (In pre-experiment, according to the visual fatigue scale, it can be determined that the 12-minute MVF induction is within the tolerance of subjects, and MVF can be formed). In the process, we use Neuroscan (an EEG acquisition equipment) to record EOG signal of all participants. Following that, another CFF was immediately measured (subjects wearing their own corrective glasses) and another EOG was recorded for 6 min after MVF. In a word, EOG data of 28 subjects were collected in 3 conditions: before MVF, during MVF induction and after MVF. CFF

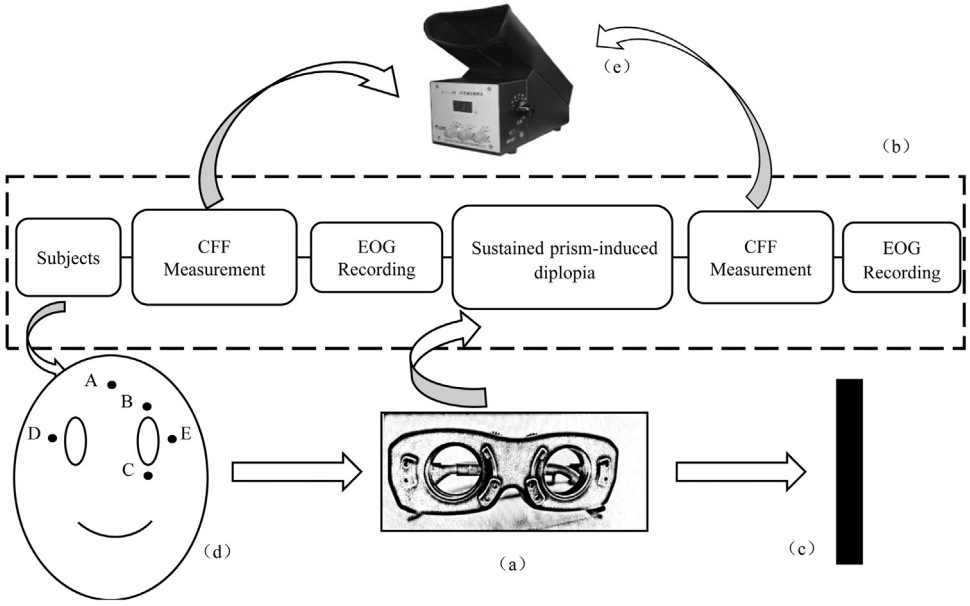

Fig. 1. The whole experimental process. (a) The glasses which are base-out and two pulleys on top of it can be used to adjust degree. The glasses are made of prism, which can be used to induce MVF in a short time. (b) The procedure of experiment and data acquisition. The procedure includes six parts: (1) Subjects: subjects preparation including facial cleaning and electrodes pasting shown as Fig. 1(d); (2) CFF Measurement: measure CFF before MVF with flash critical fusion frequency meter shown as Fig. 1(e); (3) EOG Recording: record and save EOG signals before MVF for 6 min with an EEG acquisition equipment Neuroscan; (4) Sustained prism-induced diplopia: for each subject wearing corrective glasses and prism glasses Fig. 1(a) at the same time, the prism glasses will be adjusted to a certain level to force the participants' eyes to become physiologically diplopia when they watch the 10 × 1.5 cm black line Fig. 1(c). The participants keep their eyes in this state watching the black line for 12 min to induce MVF quickly. During the induction process, EOG signals will also be recorded. (5) CFF Measurement: for each subject, after 12 min' MVF induction, we measure CFF after MVF quickly; (6) EOG Recording: after CFF measurement, EOG signals after MVF will be recorded and saved for another 6 min. (c) The vertical black line of size 10 × 1.5 cm. During MVF induction, subjects wear the adjusted prism glasses Fig. 1(a) and watch the black line Fig. 1(c) to keep physiologically diplopia for 12 min. (d) The placement of electrodes for EOG acquisition. A sketch of face is shown. The reference electrode A is located at the forehead center, electrode B is placed above the eyebrow and electrode C is located at the lower edge of the orbit. Electrodes B and C are in the same line with the eyeball. Electrodes D and E are placed in the outer edge of the left and right eye orbit and they are in the same line with the eyeball. Use electrodes B and C to collect VEOG; Use electrodes D and E to collect HEOG. (e) Flash critical fusion frequency meter to measure CFF. Use CFF meter to measure CFF before and after MVF, which can be regarded as an objective behavioral indicator for MVF detection.

of 28 subjects were measured before and after the prism-induced process.

2.3. CFF measurement

Visual acuity is one of the basic functions of eyes, which can be used as a behavioral indicator of visual fatigue [22]. As shown in Fig. 1(e), flash critical fusion frequency meter can measure the critical frequency of flash fusion and detect the level of the ability to identify the flash, and the accuracy is less than 0.1 Hz. In this experiment, we measured the CFF of the two states (before and after MVF) of the subjects by the flash fusion frequency instrument. The parameters of the flash fusion frequency meter were set as follows: brightness 1/8, background light 1/16 and bright-black ratio 1:1. For all subjects, the CFF corresponding to red light was measured and recorded. To improve CFF measurement accuracy of each state, we measured two CFF values; in the process of increasing the flash frequency, we got one CFF and the other one in the reverse process. In order to obtain the required value, these two measured CFF values were averaged.

Studies have found that CFF is negatively correlated with visual fatigue [14], so CFF can be measured to evaluate and detect MVF. Moreover, CFF can be used as a behavioral indicator to judge the effectiveness of EOG physiological indicators application in evaluating MVF.

2.4. EOG recording

During the experiment, we used Neuroscan to record EOG signal. All EOG signals were recorded from the left eye. Neuroscan is an advanced EEG/ERP acquisition analysis system with 128 channels, which can obtain EOG with high signal-to-noise ratio (SNR). The software curry8 for Neuroscan can achieve elementary data processing and analysis. The sampling frequency is 1000 HZ. The default cut-off frequency of high-pass filter is 0.5 HZ and that of low-pass filter is 100 HZ. In addition, make sure that skin impedance of each electrode is less than 20kΩ. Electrodes placement is shown in Fig. 1(d). Five AgCl electrodes form a two-channel connection. The reference electrode A is located at the forehead center, electrode B is placed above the eyebrow and C is located at the lower edge of the orbit. Electrodes B and C are in the same line with the eyeball. Electrodes D and E are placed in the outer edge of the left and right eye orbit and they are in the same line with the eyeball. When the eye moves vertically, the potential difference between B and C changes to produce vertical electrooculogram (VEOG); when the eye moves horizontally, the potential difference between D and E changes to produce horizontal electrooculogram (HEOG) [23]. Then curry8 was used to record and save the EOG data and MATLAB was used to design a band-pass filter with cut-off frequencies of 0.3 and 30 Hz to filter out the baseline drift along with high-frequency noise. Finally, we got the preprocessed EOG signal, which would be used for subsequent calculations and analysis.

2.5. Data preprocess

For CFF, we measured CFF values twice for each state (before and after MVF) of each participant and then averaged the two values to obtain CFF values of all participants. As an objective behavioral indicator, since CFF is negatively correlated with visual fatigue [14], it will be regarded as a criterion to assess the effectiveness of EOG physiological indicators for MVF detection and evaluation. For EOG, after band-pass filtering (0.3–30 Hz), we found that strong interfer-

ence still existed in one subject's EOG signals. So the remaining 27 subject's EOG signals were selected for subsequent analysis. Since frequency domain of VEOG is mainly below 10 Hz, we conducted another band-pass filtering (0.3–10 Hz) for VEOG. Furthermore, in order to process the signal faster, the signal was resampled at 128 Hz.

2.6. Calculation methods of energy ratio of low frequency to high frequency (ERLH)

Wavelet packet analysis can subdivide signals without repetition or omission on a full scale, so as to realize time-frequency localization analysis of all kinds of signals. Since different wavelet bases have different local characteristics in time domain and frequency domain, it is very important to choose the appropriate wavelet base for wavelet packet analysis. Considering that the shape of db4 wavelet base is similar to EOG spike component and the wavelet base has pretty good frequency separability, db4 is most often used in physiological signals analysis. Gradolewski considered db4 as the best wavelet to filter signal [24]. Zhou removed noise in EEG with db4 wavelet [25]. Daud carried out a time frequency analysis of EOG by using db4 as a mother wavelet [26]. When EOG decomposition level was set 10, for dbN, low-pass component has maximal energy when N = 4, so db4 was selected as the optimal wavelet base in this study [27]. At the same time, we lowered the EOG sampling rate from 1000 Hz to 128 Hz. We figured out the energy of each node based on the coefficients of wavelet packet decomposition. Firstly, a series of wavelet packet decomposition coefficients C10i (j) were obtained from the 10-level wavelet packet decomposition of the EOG signal. In C10i (j), i = 0,1,2,. . .,1023, j = 0,1,2,. . .,1023. So frequency band width of each node was (128/2 Î 1) Hz, and each node was reordered by gray code according to the frequency band order it represented. Then, wavelet packet coefficients were reconstructed. The reconstructed signals of 0–2.5 Hz could be expressed as

$$S_1(t) = \sum_{i=0}^{11} S_{10i}(t) \tag{1}$$

And that of 2.5–10 Hz could be expressed as

$$S_2(t) = \sum_{i=12}^{128} S_{10i}(t) \tag{2}$$

According to the Parseval's theorem, the signal power of each frequency band is

$$W_{10i} = \sum_{j=0}^{1023} (C_{10i}(j))^2 \tag{3}$$

Which can be obtained according to the wavelet packet decomposition coefficient and the total power W is equal to the sum of the power of each node. Therefore, ERLH of HEOG may be obtained as a physiological indicator to detect MVF [19].

2.7. Calculation methods of WPBF

Since ERLH varied greatly with individuals and the choice of frequency band would affect the result, we calculated WPBF. WPBF mainly reflects the distribution and migration of signal power spectral density, and the calculating formula is as follows:

$$f_g = \frac{PF}{P},\ \mathrm{PF} = \sum_{f=f1}^{f2} (p(f) \times f),\ P = \sum_{f=f1}^{f2} (p(f)) \tag{4}$$

In this equation, f_g is power spectrum barycenter frequency, f_1 and f_2 are frequency range values, $p(f)$ is the power spectrum of a signal and f is frequency value. Similarly, the wavelet packet decomposition coefficient is used to estimate the power of each frequency band, and the mean of each frequency band is taken as the frequency value of the node. The barycenter frequency obtained by this method is defined as WPBF. The calculating formula is as follows:

$$f_{wg} = \frac{WF}{W},\ WF = \sum_{j=0}^{i-1} \left(W_{ij} \times f_j\right),\ W = \sum_{j=0}^{i-1} W_{ij} \tag{5}$$

In which i denotes the level of wavelet packet decomposition, j is the number of nodes, W_{ij} represents the signal power of the jth node at ith level of wavelet packet decomposition and f_j represents the frequency mean corresponding to the jth node.

2.8. Extraction of blink characteristics

In order to calculate ABT and average blink energy (ABE), we need to extract blink characteristics first. In comparison between the difference method [28] and the short-time energy threshold method [29], a short-time energy threshold method based on the first-order differential of EOG was proposed. However, since the amplitudes of the signal waveforms of different subjects are different, it is necessary to set a threshold for the signal of each subject. First, the EOG signal was normalized and processed by first-order differential to obtain a differential signal v(t). Then, it was framed by moving window, and the energy E of each signal was calculated separately. By setting the threshold to E_0, if $E \geq E_0$, we would determine that this frame signal belonged to a blink signal, and then record this frame status value as 1; instead, this frame state would be recorded as 0. Then move the window continually to get the short-term energy of the next frame and compare it with the threshold. Finally, the state values of all the frames were obtained, the distance between 1 and the adjacent 0 was calculated, and converted into a time interval according to the sampling frequency of the signal. Since the above determination might have misjudgment, we made further determination according to the duration of the blinking action and the time interval between blinking actions so as to achieve the blinking feature extraction with high accuracy. The specific algorithm flow is shown in Fig. 2.

After blink features extraction, ABT and ABE can be calculated separately.

First, the EOG signal was normalized and processed by first-order differential to obtain a differential signal v(t). Then, it was framed by moving window, and the energy E of each signal was calculated separately. By setting the threshold to E0, if E ≥ E0, we would determine that this frame signal belonged to a blink signal, and then recorded this frame status value as 1; instead, this frame state would be recorded as 0. Then move the window continually to get the short-term energy of the next frame and compare it with the threshold. Finally, the state values of all the frames were obtained, the distance between 1 and the adjacent 0 was calculated, and converted into a time interval according to the sampling frequency of the signal. Since the above determination might have misjudgment, we made further determination according to the duration of the blinking action and the time interval between blinking actions so as to achieve the blinking feature extraction with high accuracy.

2.9. Calculation and statistical methods

We selected signals from 30 to 90 s for calculations with MATLAB algorithms both before and after MVF. For each state, we got ERLH and WPBF based on HEOG; also, we got ABT and ABE based on VEOG. Then spearman correlation analysis was conducted between

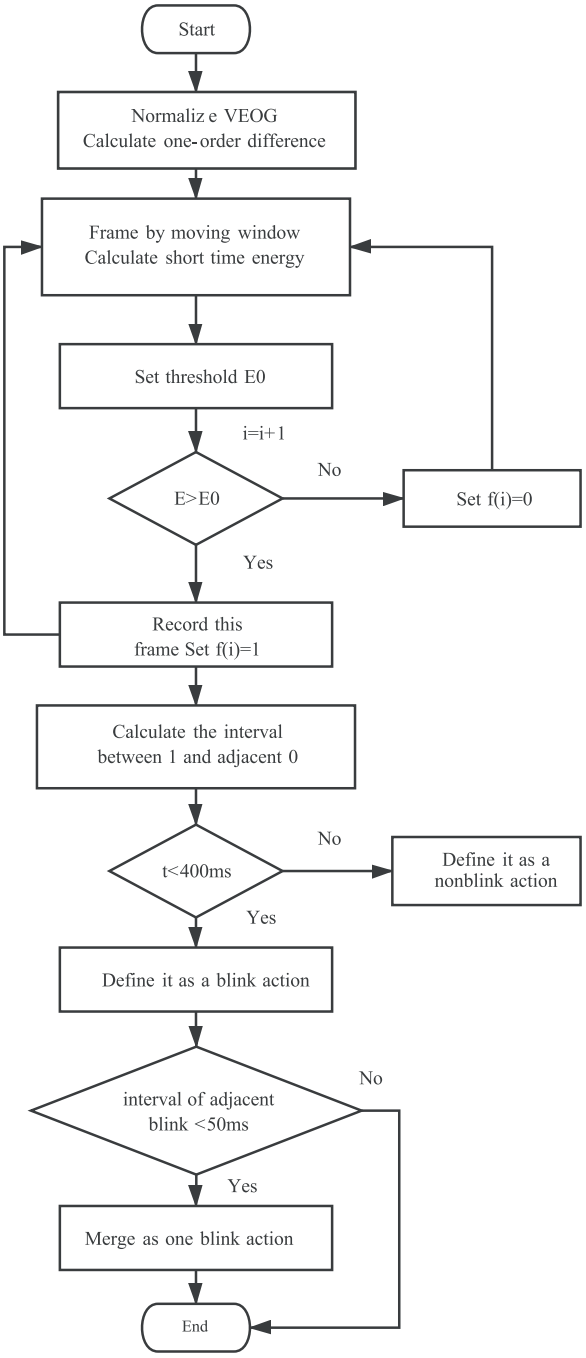

Fig. 2. Blink feature extraction process.

the above four physiological indicators and CFF values for each state. For the physiological indicators which are significantly correlated with CFF both before and after MVF, we selected signals from 2 to 11 minutes during MVF induction for each participant; then we calculated the corresponding physiological indicator with a 30-second time window (step: 15 s) and got a physiological indicator vector (1×39) for every participant; for all 27 participants, we got a physiological indicator matrix (27×39). The physiological indicator matrix was averaged by columns, and one characteristic vectors (1×39) was obtained, which was used to represent the general tendency of the corresponding physiological indicator during MVF induction. In addition, we conducted a statistical difference analysis between CFF values before and after MVF; also, for the physiological indicator matrix (27×39), a statistical difference analysis was also carried out between start column (physiological indicator for 27 participants before MVF) and end column (physiological indicator for 27 participants after MVF). Finally, we trained a SVM model to achieve a binary classification between the state before MVF and after MVF.

Table 1
Spearman correlation coefficient between Physiological indicators and CFF.

Physiological indicators	Spearman correlation coefficient (p)	
	CFF before MVF	CFF after MVF
ERLH	−0.241 (0.227)	0.143 (0.475)
WPBF	0.409 (0.034)	0.432 (0.024)
ABT	−0.458 (0.016)	−0.522 (0.005)
ABE	−0.248 (0.212)	−0.122 (0.546)

Note: significant at $p < 0.05$, otherwise, $p > 0.05$. CFF: Critical Fusion Frequency; MVF: Muscular Visual Fatigue; ERLH: Energy Ratio of Low Frequency to High Frequency; WPBF: Wavelet Packet Barycenter Frequency; ABT: Average Blink Time; ABE: Average Blink Energy.

2.10. SVM classifying

We chose the physiological indicators significantly correlated with CFF values as SVM training features. And for the corresponding physiological indicator matrix (27×39), we selected the start column (physiological indicator for 27 participants before MVF) and the end column (physiological indicator for 27 participants after MVF) as SVM training samples. Then we labeled state before MVF as −1 and state after MVF as 1. For all training samples, preprocessing including normalization and standardization was carried out. Then we adjusted SVM parameters with grid search algorithm and found that the optimal parameters were as follows: kernel function, radial basis function (RBF); regularization parameter C = 100; kernel coefficient gamma = 0.01. Finally, we applied a 9-fold stratified cross validation in the SVM training [30] and got the receiver operating characteristic (ROC) curve of each fold. By averaging all 9 ROC curves, we got a mean ROC curve. And we calculated the area under curve (AUC) of corresponding ROC curves [31].

3. Results

3.1. Correlation analysis between physiological indicators and CFF

With the statistical analysis software PASW Statistics 18.0, we performed a spearman correlation analysis between the calculated physiological indicators and CFF values both before and after MVF. Before MVF, rERLH = −0.241 ($p = 0.227$), rWPBF = 0.409 ($p = 0.034 < 0.05$), rABT = −0.458 ($p = 0.016 < 0.05$) and rABE = −0.248 ($p = 0.212$); after MVF, rERLH = 0.143 ($p = 0.475$), rWPBF = 0.432 ($p = 0.024 < 0.05$), rABT = −0.522 ($p = 0.005 < 0.05$) and rABE = −0.122 ($p = 0.546$). See the correlation analysis result in Table 1. From correlation analysis result, we can see that WPBF is significantly positive correlated with CFF both before and after MVF; and that ABT shows a significant negative correlation with CFF both before and after MVF. Since CFF, as an objective behavioral indicator for MVF detection, is negatively correlated with MVF [14], we come to a conclusion that WPBF is negatively correlated with MVF and ABT is positively correlated with MVF, i.e., physiological indicators WPBF and ABT can be used for accurate detection of MVF.

3.2. Physiological indicators tendency during MVF induction

According to the calculation methods described in 'Calculation and statistical methods', we got the general WPBF tendency (Fig. 3)

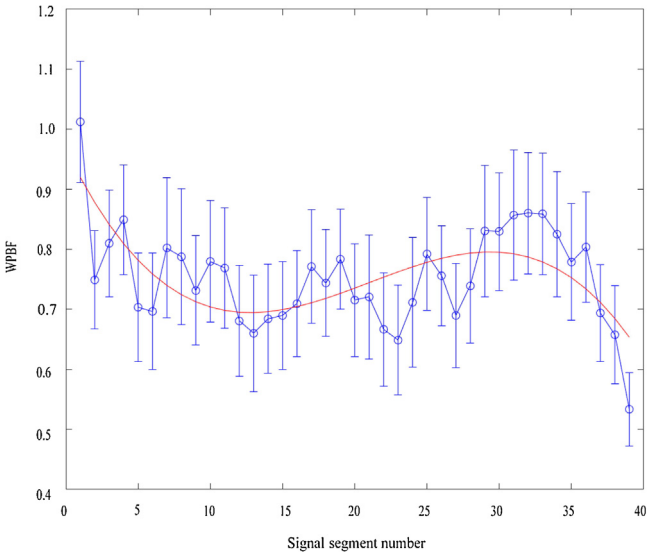

Fig. 3. The trend of WPBF over time.

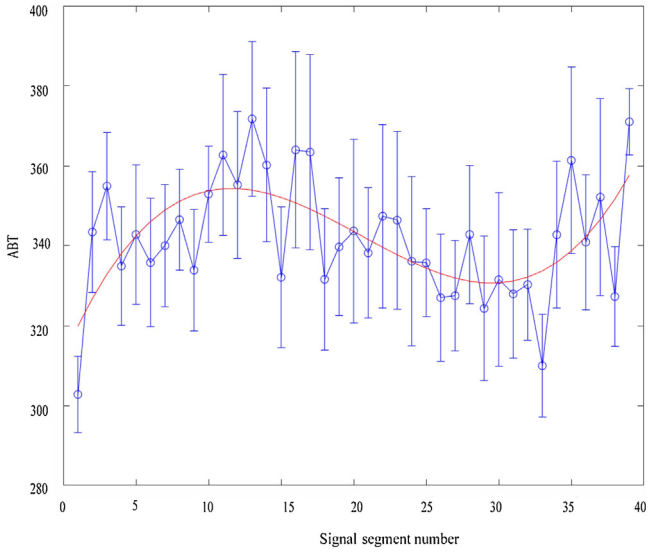

Fig. 4. The trend of ABT over time.

and ABT tendency (Fig. 4) during MVF induction. In Figs. 3 and 4, blue circle represents the mean value of each column in physiological indicator matrix (27×39), blue error bar means the standard error of each column in physiological indicator matrix (27×39) and the red curve is a cubic polynomial fitting. From Fig. 3, we see that WPBF drops as a whole when the MVF induction time gets longer; while from Fig. 4, we know that ABT rises as a whole in the same process. The results support the conclusion that WPBF is negatively correlated with MVF and ABT is positively correlated with MVF. What's more, WPBF tendency and ABT tendency have a high degree of consistency according to MVF induction time, which indicates that WPBF and ABT can be used for accurate MVF detection synthetically.

For physiological indicator WPBF, we selected signals from 2 to 11 minutes during MVF induction for each participant; then we calculated WPBF with a 30-second time window (step: 15 s) and got a WPBF vector (1×39) for every participant; for all 27 participants, we got a WPBF matrix (27×39). Blue circle represents the mean value of each column in WPBF matrix, blue error bar means the standard error of each column in WPBF matrix, and the red curve is a cubic polynomial fitting. Signal segment number: MVF induction time ranges from 1 to 39. WPBF: Wavelet Package Barycenter Frequency (unit: Hz).

Table 2
Indicators statistical difference analysis before and after MVF.

Indicators	Tests of Normality	CMT	Mean_D_Indi (p)
CFF	0.249	PST	−1.83 (0.000)
WPBF	0.113	PST	−0.48 (0.000)
ABT	0.074	PST	6.82 (0.000)

Note: for Tests of Normality, significant at $p > 0.05$; CMT: Compare Mean Type; PST: Paired Sample T Test; MVF: Muscular Visual Fatigue; Mean_D_Indi: the mean value of indicators difference between after and before MVF. For the indicators difference between after and before MVF, significant at $p < 0.05$. CFF: Critical Fusion Frequency; WPBF: Wavelet Packet Barycenter Frequency; ABT: Average Blink Time.

For physiological indicator ABT, we selected signals from 2 to 11 minutes during MVF induction for each participant; then we calculated ABT with a 30-second time window (step: 15 s) and got a ABT vector (1×39) for every participant; for all 27 participants, we got a ABT matrix (27×39). Blue circle represents the mean value of each column in ABT matrix, blue error bar means the standard error of each column in ABT matrix, and the red curve is a cubic polynomial fitting. Signal segment number: MVF induction time ranges from 1 to 39. ABT: Average Blink Time (unit: millisecond).

3.3. Indicators statistical difference analysis before and after MVF

With the statistical analysis software PASW Statistics 18.0, we also performed a statistical difference analysis for indicators CFF, WPBF and ABT before and after MVF. The tests of normality result for all indicators is $pCFF = 0.249 > 0.05$, $pWPBF = 0.113 > 0.05$ and $pABT = 0.074 > 0.05$; all indicators meet the normality tests, so we conduct the paired sample T (PST) test to compare mean. Mean_D_Indicators represents the mean value of pairwise difference between indicator vectors after MVF and before MVF. After PST analysis, we found that Mean_D_CFF = −1.83 ($p = 0.000 < 0.01$), Mean_D_WPBF = −0.48 ($p = 0.000 < 0.01$) and Mean_D_ABT = 68.21 ($p = 0.000 < 0.01$). See the indicators statistical difference analysis result in Table 2. From the result, we can see that under the criterion of 0.01 all indicators have a significant statistical difference before and after MVF; after MVF, CFF and WPBF show a significant drop while ABT shows a significant rise. The results support the conclusion that WPBF is negatively correlated with MVF and ABT is positively correlated with MVF. And the results indicate that 12-minute MVF experiment has induced MVF to a great extent.

3.4. MVF binary classification research

We chose the physiological indicators WPBF and ABT as SVM training features. For the two physiological indicators matrix (27×39), we selected the start column (physiological indicator for 27 participants before MVF) and the end column (physiological indicator for 27 participants after MVF) as SVM training samples. Then we labeled 27 training samples (WPBF, ABT) before MVF as −1 and another 27 training samples (WPBF, ABT) after MVF as 1. We normalized and standardized all training samples as (NS_WPBF, NS_ABT). Then through grid search algorithm we got the optimal SVM parameters: kernel function, radial basis function (RBF); regularization parameter C = 100; kernel coefficient gamma = 0.01. Finally, we performed the 9-fold stratified cross validation in the SVM training process and got ROC curves and AUC results. See results in Fig. 5. Fig. 5 shows the ROC curves and AUC results: ROC fold 1 (area = 1.00), ROC fold 2 (area = 0.78), ROC fold 3 (area = 0.78), ROC fold 4 (area = 1.00), ROC fold 5 (area = 1.00), ROC fold 6 (area = 0.89), ROC fold 7 (area = 0.78), ROC fold 8 (area = 0.89), ROC fold 9 (area = 1.00). We averaged the ROC curves and AUC values, as a result, we got a mean ROC curve and mean AUC value:

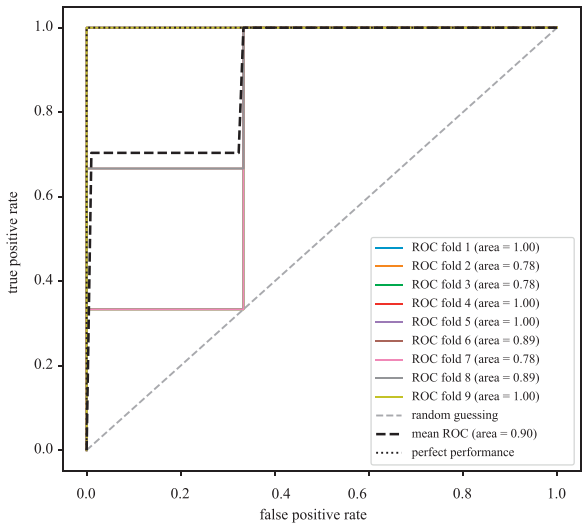

Fig. 5. the ROC curves and AUC results of 9-fold stratified cross validation Colored solid lines represent the ROC curves from fold 1 to fold 9 and we calculated the corresponding AUC: AUC fold 1 (area = 1.00), AUC fold 2 (area = 0.78), AUC fold 3 (area = 0.78), AUC fold 4 (area = 1.00), AUC fold 5 (area = 1.00), AUC fold 6 (area = 0.89), AUC fold 7 (area = 0.78), AUC fold 8 (area = 0.89), AUC fold 9 (area = 1.00). The bold dotted line shows the mean ROC curve and the corresponding mean AUC is 0.90. ROC curves of random guessing and perfect performance are also depicted in Fig. 5. ROC: Receiver Operating Characteristic curve. AUC: Area under Curve.

area = 0.90. In addition, ROC curves of classifiers with perfect performance and random guessing performance were also depicted in Fig. 5. Meanwhile, the classifier model trained through 9-fold stratified cross validation could achieve a classification accuracy of 0.796 (SD 0.172). The results support the conclusion that physiological indicators WPBF and ABT can be used for accurate detection of MVF.

4. Discussion

In our work, we used a specially designed base-out prism to induce MVF and measured EOG and the CFF values. From the results of correlation analysis between physiological indicators and CFF, we see that WPBF and ABT have a significant correlation with CFF both before and after MVF. WPBF is significantly positive correlated with CFF while ABT shows a significant negative correlation with CFF. Studies show that CFF, as an objective behavioral indicator, is negatively correlated with visual fatigue [14]. So WPBF is significantly negative correlated with MVF while ABT shows a significant positive correlation with MVF; and we conclude that physiological indicators WPBF and ABT may achieve a more accurate MVF detection in place of behavioral indicator CFF. However, for physiological indicators ERLH and ABE, there is no significant correlation with CFF; so ERLH and ABE can't be used for MVF detection.

From the results of physiological indicators tendency during MVF induction, we see that, on the whole, WPBF and ABT both change monotonically with the deepening of MVF, and the turning point appears consistently at approximately 19th signal segment, indicating that these two EOG physiological indicators are consistent in the detection and evaluation of MVF. The 19th signal segment is just the half time point (360 s) of the whole MVF induction time (720 s); and at this moment, the participants will be informed of the remaining induction time, which may cause the participants to suddenly become sober. Then the participant's increased cognitive ability may play a role in the MVF induction, so that there is a turning point at that moment.

From the results of indicators statistical difference analysis before and after MVF, we can see that CFF and WPBF show a significant drop while ABT shows a significant rise. The CFF is an effective behavioral indicator of MVF assessment [14], which measures the minimal number of flashes of light per second at which an intermittent light stimulus no longer stimulates a continuous sensation. As a highly sensitive indicator to be measured easily, the CFF is widely applied to evaluate retinal functionality. In this study, we found that the CFF significantly decreased after persistent diplopia caused by excess prism-induced disparity, which demonstrated increased MVF [22]. And the significant difference of WPBF and ABT also indicates increased MVF after the induction process.

In addition, in the research field of muscle fatigue, median frequency (MF) is often used to evaluate muscle fatigue through Electromyography (EMG). MF decreases linearly with the extension of muscle activity [32]. From the above analysis, it can be seen that during the formation of MVF, the WPBF significantly decreases, which is consistent with the results of muscle fatigue studies. So it is reasonable to apply WPBF in accurate MVF detection. Also, in many studies, eye movement indicators are used to assess visual fatigue. Eye movement parameters such as blink duration, blink frequency and pupil diameter collected by eye tracker can reflect the condition of visual fatigue. Previous studies have shown that the blink duration significantly increases after visual fatigue [33]. In this work, with the deepening of MVF, ABT becomes longer as a whole, which is consistent with the research results of visual fatigue. So it supports that ABT can also be used for MVF detection.

Moreover, from the MVF binary classification results, we see that the trained classifier model has an accuracy of 0.796 (SD 0.172) and mean AUC value: area = 0.90, which indicates a pretty well classifying performance. Also, in the MVF binary classification research, we tried different SVM parameters through grid search algorithm and found the optimal parameters. We also tried to train SVM through KFold cross validation and stratified KFold cross validation; and through 9 Fold stratified cross validation, we got the best mean AUC. So the trained classifier model can be used for MVF binary classifying, which is of great importance to prevent and treat MVF in time. To get a better classifying performance, maybe we should try to calculate some other EOG indicators and to train the classifier model with more physiological features.

There are many studies on the assessment and detection of visual fatigue. Rajabi-Vardanjani designed and validated a questionnaire for visual fatigue assessment [34]. Clavijo analyzed the blink rate to detect visual fatigue [35]. Yang studied visual fatigue based on ECG and EOG [36] and Kang did the work based on EEG [37]. However, most studies on visual fatigue are not really based on MVF caused by eye muscle fatigue. They mainly focused on visual fatigue caused by cognitive fatigue. Although EOG is directly related to eye muscle fatigue, there is no specific experimental design for eye muscle fatigue in the existing research. This study combined EOG analysis and special experimental design (base-outward prism) to rapidly induce eye muscle fatigue, providing a scientific approach for MVF study.

There are almost no studies on the pre-detection of MVF. Zeng studied MVF causes, diagnosis and surgery effect in his research [5] and Wu investigated the relationship between MVF post photorefractive keratectomy and eccentric ablation [38]. However, there is no objective pre-detection method for MVF. In this study, we induced subjects to develop symptom of slight eye muscle fatigue through the special experiment design and then acquired EOG signals that are most closely related to eye muscle fatigue. By analyzing EOG signals, we got indicators used for eye muscle fatigue detection. So during near work, once eye muscle fatigue occurs, EOG indicators will raise the alarm so as to avoid long time near work and to greatly reduce the probability of MVF. Therefore, this study is of great significance for the detection of eye muscle fatigue and the pre-detection of MVF.

5. Conclusions

From the results of correlation analysis, we conclude that physiological indicators WPBF and ABT may achieve a more accurate MVF detection in place of behavioral indicator CFF; from the results of physiological indicators tendency, we find that EOG physiological indicators WPBF and ABT are consistent in MVF detection; the results of indicators statistical difference analysis show increased MVF after the induction process; and the SVM binary classification results indicate a pretty good classifying performance for MVF. In conclusion, physiological indicators WPBF and ABT can be used for accurate eye muscle fatigue detection, which is of great importance for pre-detection and prevent of MVF. In a future study, we will try to get more physiological indicators and to validate the MVF detection results after MVF rehabilitation training.

Authors' contributions

MS, TL and JW designed the experiments. MS, LL and JG conducted the experiments. MS, LL and YW analyzed the data and interpreted the results. SL provided the base-out prism. MS wrote the manuscript and QU checked the manuscript grammar and expression. All authors read and approved the final manuscript. MS and LL contributed equally to this work and should be considered as co-first authors.

Availability of data and materials

The datasets generated and/or analyzed during the current study are not publicly available, but are available from the corresponding author on reasonable request, please contact author for data requests.

Ethics approval and consent to participate

Informed consent was obtained from all subjects of the participants, according to the Declaration of Helsinki. The ethics committees of School of Medicine, Xi'an Jiaotong University approved the study.

CRediT authorship contribution statement

Mengchuang Song: Conceptualization, Methodology, Software, Writing - original draft, Formal analysis, Investigation. **Lina Li:** Software, Formal analysis, Investigation. **Jintao Guo:** Investigation. **Tian Liu:** Conceptualization, Methodology. **Shuyin Li:** Investigation. **Yingtuo Wang:** Methodology, Formal analysis, Software.Writing - review & editing. **Jue Wang:** Conceptualization.

Acknowledgements

The study received support from the National Natural Science Foundation of China (Grant 61431012 and 61503295), the Shaanxi Province Natural Science Foundation (Grant 2018JM7080), China Postdoctoral Science Foundation (Grant No. 2018M643672) and the Fundamental Research Funds for the Central Universities (Grant xjh012019049).

Declaration of Competing Interests

The authors declared no potential conflicts of interest with respect to the research, authorship, and/or publication of this article.

References

[1] H. Simmerman, Visual fatigue, Clin. Exp. Optom. 34 (2010) 66–78.
[2] K. Kaur, H. Kaur, M.K. Sidhu, Computer vision syndrome: a major concern for VDT users, Asian J. Home Sci. (2015).
[3] Y.L. Feng, J. Dong, J.X. Tang, Z.Y. Liu, Analysis on causes of visual fatigue in 3502 cases, Int. Eye Sci. (2016).
[4] Y.H. Lin, C.-Y. Chen, S.-Y. Lu, Y.-C. Lin, Visual fatigue during VDT work: effects of time-based and environment-based conditions, Displays 29 (2008) 487–492.
[5] T. Zeng, Y. Dai, X.H. Chen, Effects of operative treatment for muscular asthenopia caused by esophoria, Int. Eye Sci. 16 (2016) 999–1000.
[6] Á. Garcíamuñoz, S. Carbonellbonete, P. Cachomartínez, Symptomatology associated with accommodative and binocular vision anomalies, J. Optom. 7 (2014) 178–192.
[7] J.C. Rucker, Overview of anatomy and physiology of the ocular motor system Handbook of Clinical Neurophysiology., vol. 9, 2010, pp. 18–42.
[8] C.A. Mayhew, The importance of accurate convergence in addressing stereoscopic visual fatigue, in: Human Vision & Electronic Imaging XX, 2015.
[9] N.K. Singh, R. Mani, J.R. Hussaindeen, Changes in stimulus and response AC/A ratio with vision therapy in convergence insufficiency, J. Optom. (2017), S1888429616300693.
[10] V. Singh, K.P.S. Malik, V.K. Malik, K. Jain, Prevalence of ocular morbidity in school going children in West Uttar Pradesh, Indian J. Ophthalmol. 65 (2017) 500–508.
[11] J. Cooper, N. Jamal, Convergence insufficiency-a major review, Optometry J. Am. Optometric Assoc. 83 (2012) 137.
[12] S. Mun, M.C. Park, S. Park, M. Whang, SSVEP and ERP measurement of cognitive fatigue caused by stereoscopic 3D, Neurosci. Lett. 525 (2012) 89–94.
[13] S. Park, M.J. Won, S. Mun, E.C. Lee, M. Whang, Does Visual Fatigue from 3D Displays Affect Autonomic Regulation and Heart Rhythm? Int. J. Psychophysiol. 92 (2014) 42–48.
[14] K. Takahashi, J. Morishita, H. Tashiro, Y. Nakamura, Objective evaluation of visual fatigue for reading of radiographs displayed on medical-grade liquid-crystal displays, Jpn. J. Radiol. Technol. 66 (2010) 1416–1422.
[15] J. Kuze, K. Ukai, Subjective evaluation of visual fatigue caused by motion images, Displays 29 (2008) 159–166.
[16] Q. Wang, Hidden information technology and data processing in drowsiness detection in normal adults based on pulse signal and ECG detection in normal adults based on pulse signal and ECG, Adv. Mat. Res. 1014 (2014) 417–420.
[17] C. Chen, W. Jing, K. Li, Q. Wu, H. Wang, Z. Qian, G. Ning, Assessment visual fatigue of watching 3DTV using EEG power spectral parameters, Displays 35 (2014) 266–272.
[18] B. Zou, L. Yue, G. Mei, Y. Wang, EEG-based assessment of stereoscopic 3D visual fatigue caused by vergence-accommodation conflict, J. Disp. Technol. 11 (2017) 1076–1083.
[19] X.Q. Huo, W.L. Zheng, B.L. Lu, Driving fatigue detection with fusion of EEG and forehead EOG, International Joint Conference on Neural Networks. IEEE (2016).
[20] B. Zou, Y. Liu, Y. Wang, Study on the saccadic eye movement metric of visual fatigue induced by 3D displays, in: Sid Symposium Digest of Technical Papers, John Wiley & Sons, Ltd, 2015.
[21] W.S.M. Sanjaya, D. Anggraeni, R. Multajam, M.N. Subkhi, I. Muttaqien, Design and experiment of electrooculogram (EOG) system and its application to control mobile robotIOP Conference Series: Materials Science and Engineering, vol. 180, 2017, 012072.
[22] Y. Ikushima, H. Yabuuchi, J. Morishita, H. Honda, Analysis of dominant factors affecting fatigue caused by soft-copy reading, Acad. Radiol. 20 (2013) 1448–1456.
[23] G. Gürkan, S. Gürkan, A.B. Uşaklı, Comparison of classification algorithms for EOG signals, 20th Signal Processing and Communications Applications Conference (2012).
[24] D. Gradolewski, P.M. Tojza, J. Jaworski, D. Ambroziak, G. Redlarski, M. Krawczuk, Arm EMG wavelet-based denoising system, International Conference on Mechatronics - Ideas for Industrial Applications. Advances in Intelligent Systems and Computing (2015).
[25] W. Zhou, J. Gotman, Removal of EMG and ECG artifacts from EEG based on wavelet transform and ICA, Annual International Conference of the IEEE Engineering in Medicine and Biology Society. IEEE Engineering in Medicine and Biology Society. Conference (2004).
[26] W.M.B.W. Daud, R. Sudirman, Time frequency analysis of electrooculograph (EOG) Signal of eye movement potentials based on wavelet energy distribution, 2011 Fifth Asia Modelling Symposium (2011).
[27] Z. Peng, G. Wang, Study on optimal selection of wavelet vanishing moments for ECG denoising, Sci. Rep. 7 (2017) 4564.
[28] R.-G. Bozomitu, New methods of detecting voluntary blinking used to communicate with disabled people, Adv. Electr. Comput. Eng. 12 (2012) 47.
[29] Y.L. Chen, T.S. Kuo, W.H. Chang, J.S. Lai, A novel position sensors-controlled computer mouse for the disabled, International Conference of the IEEE Engineering in Medicine & Biology Society. IEEE (2000).
[30] T. Alaa, Parameter investigation of support vector machine classifier with kernel functions, Knowl. Inf. Syst. 3 (2019).
[31] Tom Fawcett, An introduction to ROC analysis, Pattern Recognit. Lett. 27 (2006) 861–874.
[32] F. Hug, M. Faucher, T. Marqueste, C. Guillot, Y. Jammes, Electromyographic signs of neuromuscular fatigue are concomitant with further increase in

ventilation during static handgrip, Clin. Physiol. Funct. Imaging 24 (2004) 25–32.
[33] L.L. Wang, Y. Tu, L. Shen, Y.G. He, W. Zhang, Evaluation of visual fatigue caused by 3D display, Appl. Mech. Mater. 380-384 (2013) 1059–1063.
[34] H. Rajabi-Vardanjani, E. Habibi, S. Pourabdian, H. Dehghan, M.R. Maracy, Designing and validation a visual fatigue questionnaire for video display terminals operators, Int. J. Prev. Med. 5 (2014) 841–848.
[35] G.L.R. Clavijo, J.O. Patino, D.M. Leon, Detection of visual fatigue by analyzing the blink rate, 2015 20th Symposium on Signal Processing, Images and Computer Vision (STSIVA). IEEE (2015).
[36] X. Yang, D. Wang, H. Hu, K. Yue, Visual fatigue assessment and modeling based on ECG and EOG caused by 2D and 3D displays Sid Symposium Digest of Technical Papers, vol. 47, 2016, pp. 1237–1240.
[37] Y. Kang, D. Wang, H. Hu, X. Yang, S.C. Chiu, Compare and model multi-level stereoscopic 3D visual fatigue based on EEG Sid Symposium Digest of Technical Papers, 48, 2017, pp. 1359–1362.
[38] G. Wu, L. Xie, Z. Yao, Post-PRK muscular asthenopia and eccentric ablation, Chin. Med. J. 114 (2001) 167.